Supplement Information (SI) Appendix

Material and Methods:

Cell culture and transgenic strains. Parasite cultures were maintained in primary human foreskin fibroblasts (HFF) as previously described (1). To determine growth rates for CTG and CTG-^{DD}AP2IX-9 parasites, HFF monolayers were inoculated at a 4:1 MOI, the parasites allowed to invade for 3 h, and then shifted to pH 8.2 media plus or minus 250nM Shield-1. The parasite population in each flask was monitored in real time every 24 h for 4 days with 50 randomly selected vacuoles counted in triplicate at each time point and the values averaged.

A summary of the parent strains used and transgenic clones produced for this study is provided in Dataset S1 along with the oligonucleotide primers used for cloning. **Genomic locus epitope fusions with hemagglutinin (HA) tags**. *Toxoplasma* ApiAP2 factors, AP2IX-9 (TGME49_306620) and AP2VI-1 (TGME49_240460), were tagged at the endogenous locus with a triple copy of the HA epitope in the Type II Prugniaud strain lacking the *KU80* gene (designated in this study as the PruQ strain) by genetic knock-in using the pLIC-HA3x plasmid as described in (2). **Conditional expression model.** For conditional expression, the AP2IX-9 single exon coding region was PCR amplified from genomic DNA to incorporate in frame Mfe1/Sbf1 sites, which were used to clone the purified PCR fragment into the pCTDDHA3x plasmid provided by Dr.Striepen, University of Georgia (3). This cloning results in the fusion of the FKBP peptide (11.2 kDa) and 3 copies of the HA epitope for detection (4.4 kDa) in frame with the N-terminal end of AP2IX-9 protein with a final fusion protein mass of ~128kDa (designated ^{DD}AP2IX-9). The plasmid pCTDDHA3x-AP2IX-9 was introduced by electroporation into the Prugniaud strain (wild type for *KU80*), and also into a Prugniaud transgenic clone, PruIC2, expressing firefly luciferase under the BAG1 promoter (see details of the PruIC2 strain in Appendix ref 4). Transgenic parasites were selected using chloramphenicol (20μM) and clones were isolated by limiting dilution. To produce Type III CTG parasites expressing the conditional DDHA3x-AP2IX-9 allele (^{DD}AP2IX-9), the pCTDDHA3x-AP2IX-9 plasmid was digested with SpeI/NotI to remove the sagCAT selectable marker and this was switched with the DHFR-TS selectable marker from the pT7S4HA plasmid. The resulting pDHFR/DDHA3x-AP2IX-9 plasmid was introduced by electroporation into low passage CTG strain parasites, selected with pyrimethamine (1μM) and resistant clones isolated by limited dilution. ***AP2IX-9* gene knockouts.** Transgenic parasites carrying a deletion of the *AP2IX-9* gene were obtained in the PLK, CTG-^{DD}AP2IX-9 transgenic, and the RH*ΔhxgprtΔuprt* strains as follows. To generate the PLK-Δap2IX-9 transgenic strain the pTCY plasmid (a kind gift from Dr. Striepen, University of Georgia) was first modified to expand the multiple cloning sites surrounding the sagCAT selectable marker (5' KpnI-ApaI-XhoI-SalI-ClaI-HindIII--sagCAT--3'AatII-SmaI-AvrII-NheI-BglII-SpeI) to generate the pTCY-exMCS vector. The plasmid pTCY-AP2IX-9KO was then constructed in this new vector by cloning the 5' and 3' flanking regions of the single AP2IX-9 coding exon. A 3,067bp PCR product (primer sequences are listed in Dataset S1) amplified from Prugniaud Type II strain genomic DNA supplied the left arm using KpnI/HindIII to clone and a 1960bp PCR fragment down stream of the single AP2IX-9 exon was cloned by AatII/SpeI sites in order to supply the right arm. The resulting pTCY-AP2IX-

9KO plasmid was electroporated into PLK strain, transgenic parasites selected using chloramphenicol (20μM), and cloned by limiting dilution. To produce CTG-Δap2IX-9-[^{DD}AP2IX-9] parasites the sagCAT selectable marker in pTCY-AP2IX-9KO was swapped with a phleomycin (Ble) expression cassette using PCR using HindIII/AvrII sites to generate the plasmid pT(ble)Y-AP2IX-9KO. This Ble knockout plasmid was electroporated into CTG-^{DD}AP2IX-9 parasites, subjected to two rounds of extracellular phleomycin (50μg/ml) selection and resistant parasites cloned by limiting dilution. Finally, to generate an AP2IX-9 knockout in the RH*ΔhxgprtΔuprt* strain, cosmid TOXP727 containing the AP2IX-9 locus was modified by recombineering to delete the single AP2IX-9 exon as previously described (5). The resulting TOXP727-AP2IX-9KO cosmid was electroporated into RH*ΔhxgprtΔuprt* strain, selected in chloramphenicol and resistant clones isolated by limiting dilution.

Immunofluorescence assays (IFA). Parasites were inoculated on confluent HFF coverslips for indicated time and IFA assays performed as previously described (6) using the following primary reagents: anti-HA antibody (Roche; rat mAb 3F10; 1:500), biotin-labeled *Dolichos biflorus* agglutinin (1:3000, Vector labs, CA), and DAPI (0.5mg/ml). All Alexa (Molecular Probes, CA) and streptavidin (Vector Labs, CA) conjugated secondary antibodies were used at 1:1000. Image acquisition was performed on a Zeiss Axiovert microscope equipped with 100x objective.

For IFA analysis of *in vivo* tissue cysts from murine brain, glass cover slips were treated with 1% polylysine for 20 min and then washed with PBS. Tissue cysts were placed on the cover slips and left at room temperature (RT) for 15 min followed by incubation with trypsin solution (4μl of a 1mg/ml solution, Sigma-Aldrich) for 4 min at RT. Cover slips were then fixed 4% paraformaldehyde for 30 min, washed with PBS and permeabilized with 0.2% Triton X-100 for 20 min. Lastly, cover slips were blocked with 3% BSA and 5% goat serum overnight at 4°C. IFA was preformed using the following antibodies at 37^{0}C for 90 min: HA (Roche; rat mAb 3F10, 1:500) and articulin 4 (polyclonal mAb, Dr Louis Weiss, 1:500) and visualized using Alexa-conjugated secondary antibodies at 1:1000 (Molecular Probes).

Production and purification of cysts: Mice (Balb/c^{DM1}) were infected by i.p. with 1x10^4 parasites and 2 days post-inoculation Sulfamerazine (30mg/l, Sigma-Aldrich) was added to the drinking water for the duration of the experiment. Four weeks after infection, mice were sacrificed and the cysts were purified from brain tissues as follows: Five mouse brains were washed with 10 ml PBS, placed in 10 ml 0.9% NaCl and homogenized with a potter glass homogenizer. The homogenized tissue was layered on top of 25 ml Percoll buffer (45 ml Percoll solution and 55 ml PBS) in a 50 ml centrifugation tube and separated by centrifugation (20 min at 1,500 rpm, 4^{0}C). After centrifugation, 20 ml of the middle layer solution containing the cysts was transferred to a new 50 ml tube. Cysts were washed with 30 ml of PBS by centrifugation (10 min, 750 rpm, 4^{0}C). The resulting pellet was resuspended in 1 ml PBS and cyst number quantified by light microscopy.

Western analysis. Freshly needle passed and filtered parasites were collected by centrifugation and total lysates made by boiling for 10 min at 95^{0}C in Laemmli buffer (6). Each lane on a SDS-PAGE gel was loaded with 25x10^6 parasites, separated by electrophoresis and transferred to a nitrocellulose membrane.

The blots were probed with anti-HA (Roche, 3F10, 1:500) for AP2IX-9^{HA} or ^{DD}AP2IX-9 stripped with Ponceau S (0.1%) and re-probed with anti-TgPCNA1 (1:1000)(7) to monitor nuclear TgPCNA1 as a loading control. Proteins were detected with HRP-conjugated secondary antibodies (Jackson ImmunoResearch, PA) and visualized using enhanced chemiluminescence reaction.

Electrophoretic mobility shift assays (EMSA). Complementary single stranded DNA oligonucleotides that included a 5'-biotinylated nucleotide were annealed to produce DNA probes from 35-65bp in length. Standard binding reactions were carried out at RT for 20 min using 20fmol of biotinylated DNA probe and varying concentrations of GST-AP2IX-9 protein (70-900ng) according to manufacturer's protocol (Pierce, IL). Non-biotinylated competitor DNA probes were added at 100-300x concentrations as indicated. Complexes were resolved on 6% PAGE gel, transferred to nylon membrane and detected according to manufacturer's protocol (Pierce, IL). All EMSA oligonucleotides are listed in Dataset S1.

Luciferase assays. Luciferase assays were performed according to manufacturers protocols (Promega, Madison, WI) with modifications as previously described (4). Briefly, HFF cells in T25cm^2 flasks were inoculated with PruIC2 parent or PruIC2-^{DD}AP2IX-9 transgenic parasites at 3:1 MOI, parasites were allowed to invade for 3 h, and the culture media changed to either pH 8.2 or 7.0 media plus or minus 200nM Shield-1 (Clontech). The alkaline-shifted cultures were grown in non-CO_2 conditions for 72 h and then harvested for whole cell lysates according to manufacturers protocols. Each experimental condition was assessed in three independent cultures with average statistical significance for parental PruIC2 compared to the PruIC2-^{DD}AP2IX-9 transgenic strain determined by the unpaired t-test. Average luminometer values for the results shown in Figure 4B: PruIC2 parent grown as tachyzoites=674 light units; pH 8.2 media alone=284,476 units; pH 8.2 plus Shield-1=327,870 units. PruIC2-^{DD}AP2IX-9 parasites grown as tachyzoites=216 units; in pH 8.2 media alone=56,574 units; in pH 8.2 media plus Shield-1=11,839.

Chromatin immunoprecipitation and quantitative PCR. Chromatin-immunoprecipitation (ChIP) was performed by published methods (8) with the following modifications. Following intracellular formaldehyde crosslinking and purification of the nuclear fraction, lysed nuclear material was subjected to sonication (Misonix S-4000, cuphorn probe, 30min at 80% amplitude, 30sec ON/OFF pulse) to produce 200-1000bp fragments. The soluble fraction was then isolated by centrifugation at 4°C and pre-cleared with protein-G dynabeads (Dynabeads, Invitrogen) before overnight incubation with rabbit anti-HA antibody (5µg, ab9110; Abcam). Anti-HA-DNA complexes were purified using protein-G coupled magnetic beads (Dynabeads, Invitrogen) for 1 h at 4°C, subjected to salt and lithium chloride washes and incubated overnight at 65°C in 1%SDS/TE to reverse cross-links. Samples were treated with RNase cocktail (Ambion) prior to standard phenol-chloroform extraction and DNA precipitation with ethanol. Whole genome amplification (Sigma-Aldrich) was performed on ChIP-DNA and purified using Qiagen Mini-Elute PCR Kit. Quantitative PCR (qPCR) was performed on amplified ChIP-DNA (20ng/rxn) using Fast SYBR© green master mix on an ABI 7900 according to manufacturers protocols. All qPCR DNA probes were designed using Primer3 software (9) and amplified 75-364bp fragments. The primer sequences can be found in Dataset S1. Here, ChIP was performed ^{DD}AP2IX-9 (specific chromatin) or parent strains (non-specific chromatin). Relative enrichment

values were determined using the equation $2^{-(\Delta Ct\ target - \Delta Ct\ non\text{-}target)}$ where the change in Ct value of specific versus nonspecific chromatin at target and non-target loci was calculated.

***SI Appendix* reference list.**

1. Striepen B & Soldati D (2007) Genetic manipulation of *Toxoplasma gondii*. *Perspectives and methods*, eds Weiss LM & Kim K (Academic Press, London), pp 391-418.
2. Huynh MH & Carruthers VB (2009) Tagging of endogenous genes in a *Toxoplasma gondii* strain lacking Ku80. *Eukaryot Cell* 8(4):530-539.
3. Meissner M & Soldati D (2005) The transcription machinery and the molecular toolbox to control gene expression in *Toxoplasma gondii* and other protozoan parasites. *Microbes Infect*.
4. Behnke MS, Radke JB, Smith AT, Sullivan WJ, Jr., & White MW (2008) The transcription of bradyzoite genes in *Toxoplasma gondii* is controlled by autonomous promoter elements. *Mol Microbiol* 68(6):1502-1518.
5. Brooks CF*, et al.* (2010) The *Toxoplasma* apicoplast phosphate translocator links cytosolic and apicoplast metabolism and is essential for parasite survival. *Cell Host Microbe* 7(1):62-73.
6. Suvorova ES, Lehmann MM, Kratzer S, & White MW (2012) Nuclear actin-related protein is required for chromosome segregation in *Toxoplasma gondii*. *Mol Biochem Parasitol* 181(1):7-16.
7. Guerini MN, Que X, Reed SL, & White MW (2000) Two genes encoding unique proliferating-cell-nuclear-antigens are expressed in *Toxoplasma gondii*. *Mol Biochem Parasitol* 109(2):121-131.
8. Gissot M, Kelly KA, Ajioka JW, Greally JM, & Kim K (2007) Epigenomic modifications predict active promoters and gene structure in *Toxoplasma gondii*. *PLoS Pathog* 3(6):e77.
9. Rozen S & Skaletsky H (2000) Primer3 on the WWW for general users and for biologist programmers. *Methods Mol Biol* 132:365-386.
10. Behnke MS*, et al.* (2010) Coordinated progression through two subtranscriptomes underlies the tachyzoite cycle of *Toxoplasma gondii*. *PLoS One* 5(8):e12354.
11. Altschul SF, Wootton JC, Zaslavsky E, & Yu YK (2010) The construction and use of log-odds substitution scores for multiple sequence alignment. *PLoS Computational Biology* in press.
12. Bohne W & Roos DS (1997) Stage-specific expression of a selectable marker in *Toxoplasma gondii* permits selective inhibition of either tachyzoites or bradyzoites. *Mol Biochem Parasitol* 88(1-2):115-126.
13. Bohne W*, et al.* (1998) Targeted disruption of the bradyzoite-specific gene BAG1 does not prevent tissue cyst formation in *Toxoplasma gondii*. *Mol Biochem Parasitol* 92(2):291-301.

***SI Appendix* Figures**

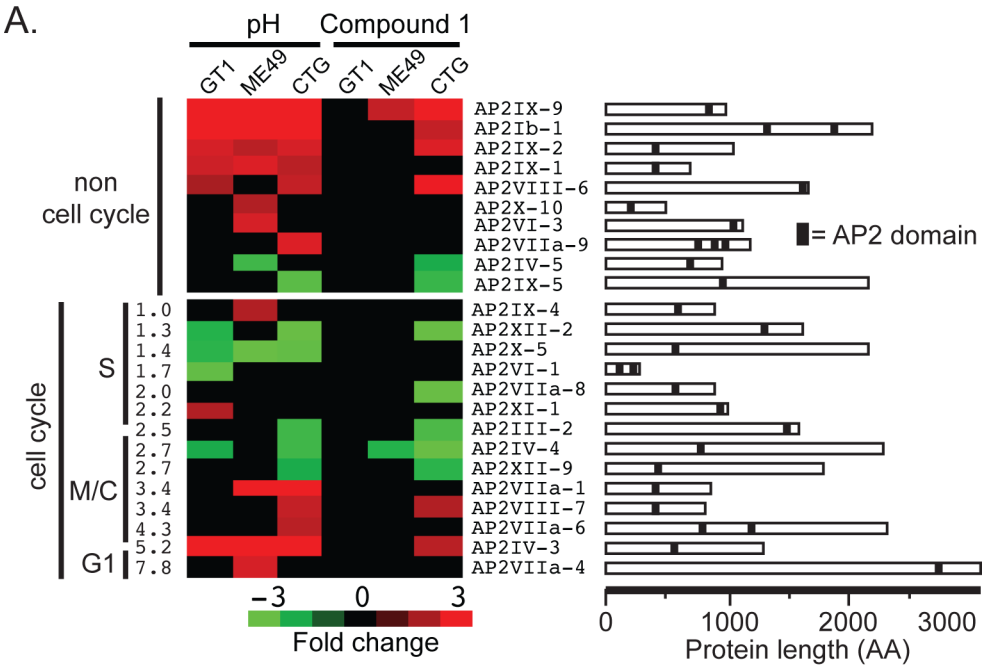

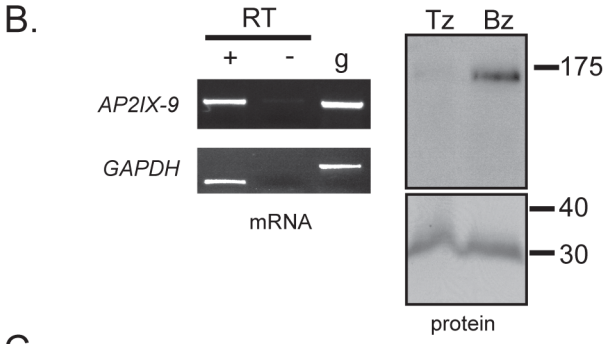

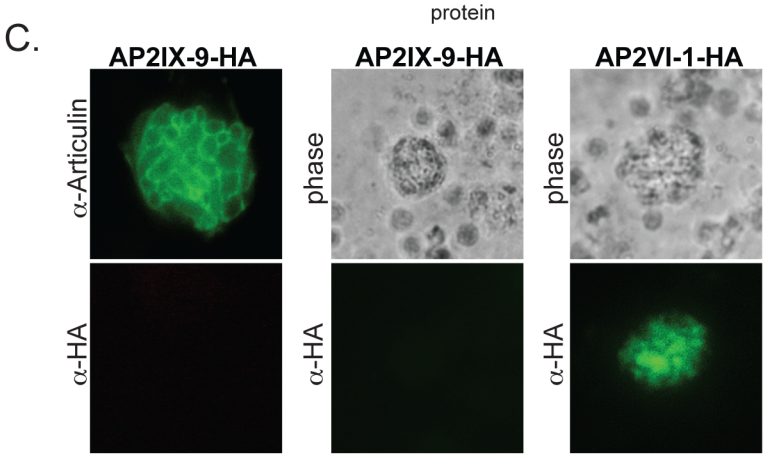

Figure S1. The expression of 24 ApiAP2 mRNAs regulated (up and down) during *in vitro* tachyzoite to bradyzoite development.

(A) Heatmap showing mRNA levels for ApiAP2 mRNAs that have >2 fold change in alkaline media (pH 8.2) and/or compound 1 (3 μM) bradyzoite induction conditions in at least one of three major genetic lineages (Type I=GT1, Type II=ME49, Type III=CTG; for microarray dataset see ref 4). Relative mRNA levels obtained from bradyzoite-induced cultures compared to the mRNA level in the matching tachyzoite strain are shown. Fold change color scale is indicated: green=downregulated; red=upregulated; black=no mRNA change compared to tachyzoites. Fourteen of these AP2s were previously identified as periodic in the tachyzoite cell cycle (10). Note that 13 of 14 cell cycle AP2s with modulated expression (up or down) during bradyzoite differentiation had maximum mRNA levels in late S to mitotic periods of tachyzoite replication (cell cycle peak times indicated on left, see also ref 10). The predicted protein sizes with the position of the ApiAP2 domain(s) indicated by black boxes for all included proteins are indicated (11). **(B) mRNA panel:** AP2IX-9^{HA} mRNA could be detected in alkaline-induced PruQ-AP2IX-9^{HA} clones (48 h in pH 8.2 media). AP2IX-9 primers are designed from a single exon, while GAPDH mRNA primers span a 432bp intron (TGME49_089690) (See Dataset S1 for primer designs). PCR fragments generated for *GAPDH* were included as loading and template quality controls. The presence of a larger GAPDH PCR fragment would indicate possible genomic DNA contamination (g lane indicates the genomic DNA fragment size), as the smaller *GAPDH* fragment is produced only from mRNA sequence. The absence of bands in the no reverse transcriptase controls (lane -) also indicate the RNA templates were DNA-free. **Protein panel**: AP2IX-9^{HA} tagged protein (endogenous promoter control) was highly expressed only in alkaline-stressed PruQ-AP2IX-9^{HA} transgenic parasites (lane Bz=72h post-infection in pH 8.2 media) and not in PruQ-AP2IX-9^{HA} tachyzoites (lane Tz=24 h post-infection in pH 7.0 media). Staining for *Toxoplasma* nuclear protein TgPCNA1 is included as a loading control. Molecular mass standards (kDa) are indicated to the right. Note AP2IX-9^{HA} is a larger mass than currently annotated (ToxoDB.org; 112 kDa prediction plus 4.4kDa 3xHA tag) due to mis-prediction of an intron, which was confirmed by sequencing of AP2IX-9 cDNA fragments (not shown). **(C)** PruQ transgenic clones epitope tagged with 3xHA by genetic knock-in at the endogenous AP2IX-9 or the AP2VI-1 locus were used to individually infect mice. At four weeks post-infection murine brain cysts were purified for immunofluorescent analysis of expression (see *SI Appendix* Methods for full details). No expression of AP2IX-9^{HA} was observed in any tissue cyst, while all cysts stained positive for AP2VI-1^{HA}. Antibodies against mouse α-articulin 4 included here allow visualization of the parasite tissue cyst and was used as a co-stain in AP2IX-9^{HA} IFAs.

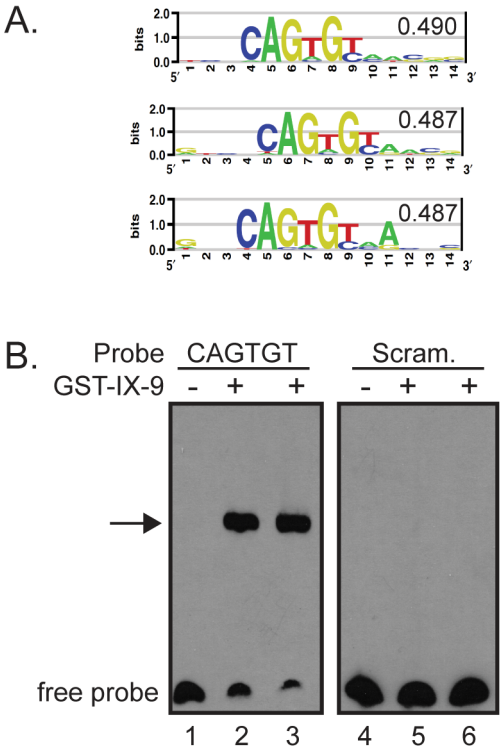

Figure S2. AP2IX-9 binds to DNA with sequence specificity.

(A) Sequence logo representation of the position weight matrices generated by the Seed and Wobble algorithm from probing an Agilent DNA microarray with purified GST-IX-9 protein (see *SI Appendix* Methods). The three related DNA motifs identified a 6 bp consensus sequence 5'-CAGTGT-'3 (3'-GTCACA-5' opposite strand sequence). **(B)** An electrophoretic mobility shift assay was performed with 0, 0.5 and 2.5 µg of purified GST-IX-9 protein and 20 fmol of 59bp 5'-biotin-labeled probe containing the CAGTGT motif or a scrambled probe (Scram; see Dataset S1 for all sequence designs). The arrow denotes a single band with slower electrophoretic migration only observed when GST-IX-9 is incubated with the CAGTGT but not the scrambled probe.

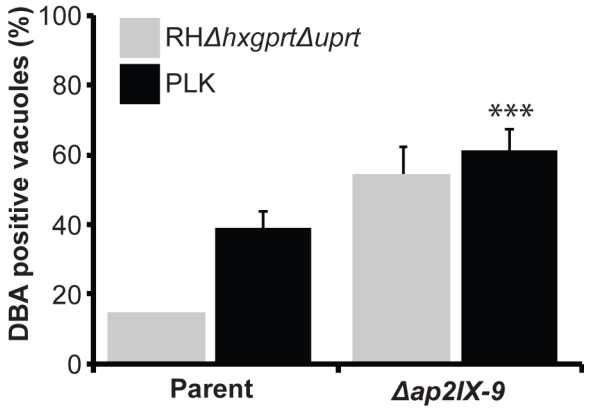

Figure S3: Targeted disruption of the *AP2IX-9* gene in laboratory strains increases tissue cyst formation in alkaline media.

Dolichos bifluorus agglutinin (DBA) positive vacuoles in RH*Δhxgrt,Δuprt,Δap2IX-9* and PLK*Δap2IX-9* transgenic parasites after *in vitro* bradyzoite induction were counted in triplicate. Tissue cyst number was determined after 4 days of CO2 starvation for the RH*ΔhxgrtΔuprt* strain background or 3 days in alkaline media (pH 8.2) media for the PLK strains. Results reflect the average of two independent clones in each knockout strain. Tissue cyst counts for the parent strains RH*ΔhxgrtΔuprt* (12) and PLK (13) are included. The legend indicates strain genetic background; RH*ΔhxgrtΔuprt*=grey bars, PLK=black bars. Statistical significance compared to parental strain was determined using the unpaired two-tailed Student's t-test (***: p-value =0.006).

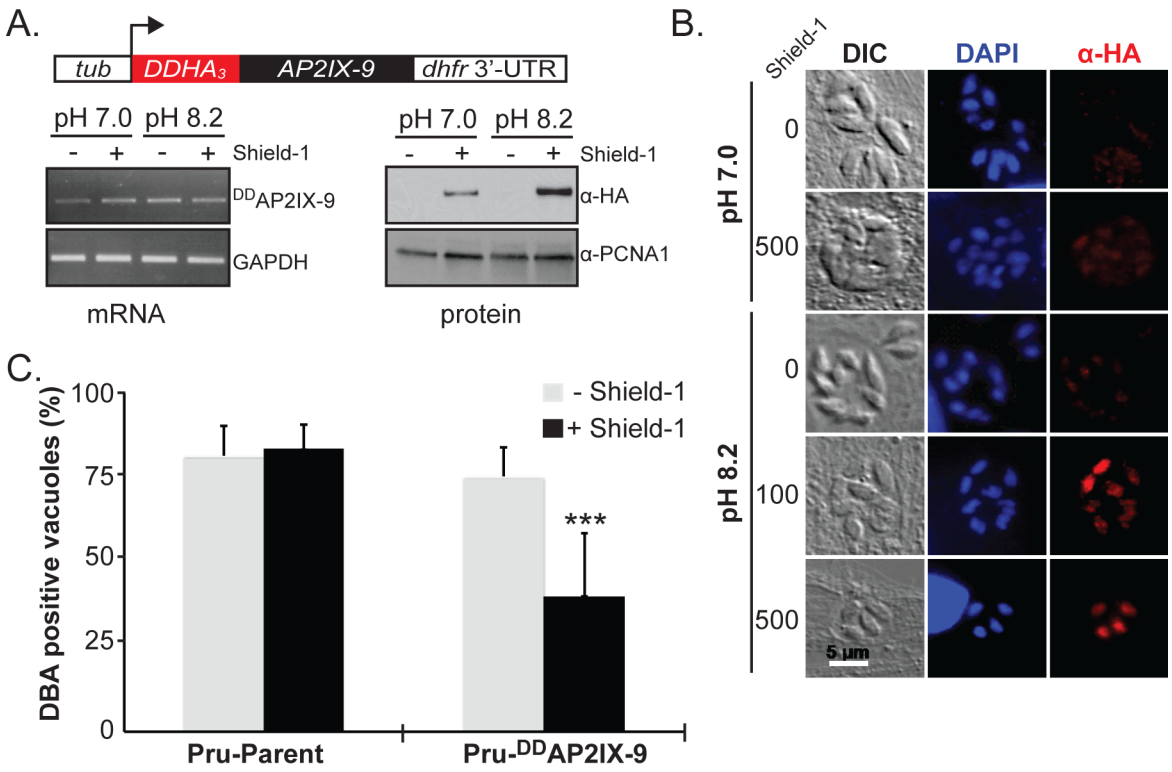

Figure S4. The development of a conditional expression model for AP2IX-9 in the Prugniaud strain. **(A)** Schematic of the AP2IX-9 conditional expression design. The DDHA3x sequence was N-terminally fused to the single coding exon of AP2IX-9 (designated ^{DD}AP2IX-9). The construct was driven by the *Toxoplasma* α-tubulin promoter and terminated with the DHFR-TS 3'-untranslated region. The ^{DD}AP2IX-9 expression construct was transfected into the Prugniaud strain (Pru; wild type for the *KU80* gene) and stable clones obtained under chloramphenicol selection in the absence of Shield-1. **(mRNA panel)** Total RNA purified from Pru-^{DD}AP2IX-9 parasites was reverse transcribed and relative levels of mRNA compared following limited PCR with primers specific for the ^{DD}AP2IX-9 transgene. Expression was assessed in parasites cultured under tachyzoite (pH 7.0 for 24 h) and alkaline induction conditions (pH 8.2 for 48 h) with or without 100nM of Shield-1. Constitutive GAPDH mRNA was included as a control and was evaluated as in Figure S1. **(protein panel)** Following a limited invasion (3 h), Pru-^{DD}AP2IX-9 parasites were shifted into alkaline media (pH 8.2 lanes) for 72h plus or minus 250nM Shield-1 and compared to parasites grown in standard pH 7.0 media (24 h growth +/- Shield-1). Note that ^{DD}AP2IX-9 expression was detected in parasites grown in either media condition when Shield-1 was added especially in pH 8.2 media, which combines natural and Shield-1 influences leading to sustained high levels of ^{DD}AP2IX-9. Each gel lane was loaded with $25x10^6$ purified parasites lysed in SDS-PAGE buffer. Following transfer to nitrocellulose the membrane was probed with anti-HA antibody, stripped and re-probed with a rabbit anti-PCNA1 antibody as a loading control. **(B)** Pru-^{DD}AP2IX-9 parasites were cultured in tachyzoite (pH 7.0 media for 24 h) or bradyzoite-induction conditions (pH 8.2 for 72 h) plus or minus Shield-1 (0, 100nM, 500nM) and then examined by immunofluorescence for ^{DD}AP2IX-9 expression (red). Red stain=anti-HA antibody and blue=DAPI staining. DIC images are shown for reference with scale bar=5 µm. **(C)** Expression of

^{DD}AP2IX-9 reduces the occurrence of tissue cysts *in vitro*. HFF cells were grown on glass coverslips and parasites allowed to invade for 3 h (1:1 MOI). Pru-^{DD}AP2IX-9 parasites were pretreated for 6 h with 250 nM Shield-1 prior to shifting the cultures into pH 8.2 media with (black bars) or without (grey bars) 250nM Shield-1 for 72h. Induction of tissue cysts by pH 8.2 media in the Pru-parental strain was robust and unaffected by Shield-1 addition. All experimental conditions were run in triplicate with 50 vacuoles/experiment counted and scored for a full DBA staining. The average results from two independent transgenic clones (A6 and B4) are shown. A significant 2-fold difference in tissue cysts number was observed between the Pru-parent and Pru-^{DD}AP2IX-9 parasites (Student's two-tailed t-test, *** p-val <0.001).

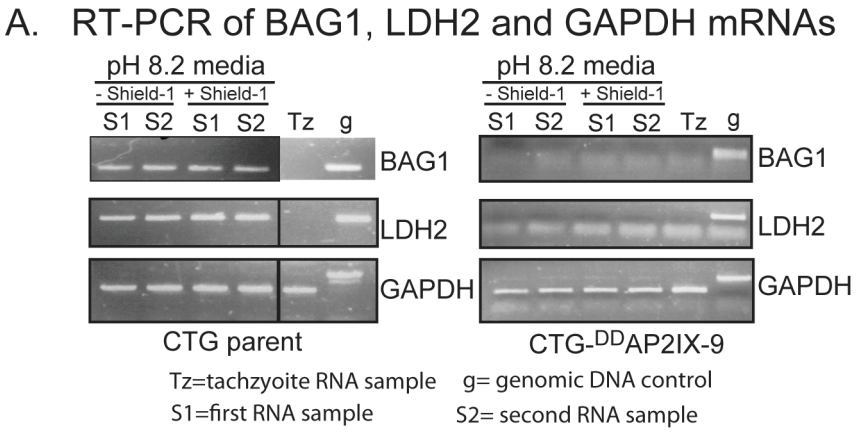

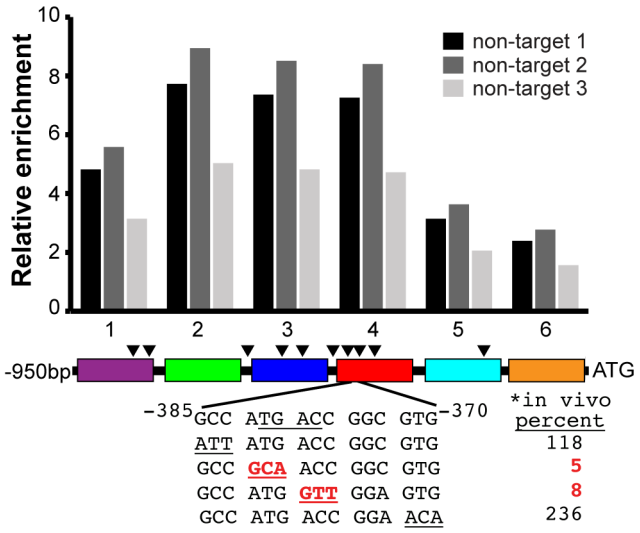

Figure S5. AP2IX-9 overexpression inhibits bradyzoite gene expression through direct promoter interaction.

(A) To validate the microarray results in Figure 4A, duplicate total RNA samples (S1 and S2) from the CTG or CTG-^{DD}AP2IX-9 parasites were purified and analyzed for BAG1 and LDH2 mRNAs as well as control GAPDH mRNA by semi quantitative RT-PCR. Following stimulation with pH 8.2 media (plus or minus Shield-1) BAG1 and LDH2 mRNAs were detected in CTG parent RNA, but not from CTG-^{DD}AP2IX-9 RNA. Consistent with induced expression only during bradyzoite differentiation, BAG1 and LDH2 mRNAs were also not detected in tachyzoite RNA samples (Tz), while the constitutively expression GAPDH mRNA was detected in all RNA samples. The lack of BAG1 and LDH2 mRNA expression detected in CTG-^{DD}AP2IX-9 parasites by the RT-PCR here is comparable to the low RMA values observed for the CTG-^{DD}AP2IX-9 samples in the microarray analysis (see Dataset S1 for RMA values). Generally, fold change determined from microarray analysis when RMA values fall near or below the fluorescent background of the GeneChip (50-100 RMA) poorly estimate the actual mRNA change as occurs for the repression of the BAG1 and LDH2 mRNAs in these experiments. A genomic DNA reference (g) was included here as control. Note that intron containing fragments are larger for GAPDH and BAG1, while LDH2 primers did not span an intron (see Dataset S1 for primer designs). The lower diffuse bands in the ^{DD}AP2IX-9 transgenic PCR reactions are primer-dimers that form in the absence of real product. Shield-1 (200nM) additions are indicated above each lane. **(B)** ^{DD}AP2IX-9 is enriched at the BAG1 promoter. Chromatin immunoprecipitation was performed using anti-HA antibodies on ^{DD}AP2IX-9 (specific chromatin) and parent strains (non-specific chromatin). Equal amounts of specific or nonspecific chromatin were subjected to quantitative-PCR at six target regions (1-6) tiled across the BAG1 promoter and compared to three non-target loci within the genome (Non-target 1=TgME49_chrVI, 1,281,571-1,281,849bp, non-target 2=TgME49_chrIa: 31,895-32,259bp, non-target 3=TgME49_chrVI: 1,595,703-1,596,052bp). Relative enrichment values for each BAG1 promoter region was determined as the change in Ct value of specific versus nonspecific chromatin at target and non-target loci, using the equation $2^{\wedge -(\Delta Ct\ target - \Delta Ct\ non\text{-}target)}$. The relative enrichment was calculated for each target region of the BAG1 promoter versus each individual non-target region and all showed similar DNA enrichment patterns. The average of BAG1 enrichment against all three non-target chromosome sites is presented in Figure 4D. The diagram below shows the arrangement of the six BAG1 promoter regions (-950bp to translation start indicated by arrow) with triangles above showing placement of AP2IX-9 motifs in the promoter. The results of published promoter mutagenesis that localizes the BAG1 CRE to region 4 and the specific mutations in the BAG1 promoter with reference to the results of luciferase reporter activity (*_in vivo_*, promoter mutations are underlined)(4).